Gümüşhane University Journal of Science and Technology

GUFBD / *GUJS* (2026) 16(4): 1073-1088 doi: 10.17714/gumusfenbil.1922497 Research Article

# Fairness-constrained sum-rate maximization in indoor MU-MISO VLC systems: a comparative study of RSMA, NOMA, and SDMA

**Yasin ALTUNBAŞ*[1], Kadir TÜRK[2]**

[1]*Erzincan Binali Yıldırım University, Faculty of Engineering and Architecture, Department of Electrical and Electronics Engineering, 24002, Erzincan*

[2]*Karadeniz Technical University, Faculty of Engineering, Department of Electrical and Electronics Engineering, 61080, Trabzon*

• Received: 03.04.2026 • Accepted: 27.09.2026

**Abstract**

Visible light communication (VLC) has emerged as a strong candidate for beyond-5G and 6G systems due to its capability of providing both illumination and high-speed data transmission within the visible spectrum. Nevertheless, achievable rates in practical implementations are constrained by the modulation bandwidth limitations of light-emitting diodes (LEDs). To address the growing demand for higher data rates and efficient multi-user (MU) communication, advanced multiple access (MA) schemes must be investigated for indoor VLC systems. In this paper, sum-rate maximization problems are formulated for rate-splitting multiple access (RSMA), space-division multiple access (SDMA), and non-orthogonal multiple access (NOMA) by considering practical constraints such as fairness, providing a comprehensive fairness-constrained comparison that addresses a gap in the existing VLC literature for indoor MU-MISO systems. The resulting optimization problems are non-convex in nature. To solve these problems, particle swarm optimization (PSO) is utilized as a meta-heuristic approach. All numerical simulations are conducted in MATLAB. Numerical results demonstrate that RSMA achieves sum-rate performance comparable to NOMA while consistently outperforming SDMA, particularly in overloaded scenarios where SDMA cannot maintain reliable transmission. Furthermore, RSMA can achieve stable sum-rate performance under various fairness constraints, unlike NOMA and SDMA, whose performances fluctuate greatly depending on different fairness requirements and user distribution scenarios. Moreover, the performance gaps among RSMA, SDMA and NOMA can be more pronounced under different fairness constraints, which shows the robustness of RSMA for fairness-aware indoor MU-MISO VLC systems.

**Keywords:** Fairness, Non-orthogonal multiple access (NOMA), Rate-splitting multiple access (RSMA), Space-division multiple access (SDMA), Visible light communication (VLC)

## 1. Introduction

The demand for high-speed wireless communication has significantly increased in recent years. However, the limited capacity of the conventional radio frequency (RF) spectrum makes it challenging to satisfy requirements. For this reason, alternative communication technologies have attracted considerable attention from both academia and industry. Visible light communication (VLC) is regarded as a promising substitute for RF systems among optical wireless communication (OWC) technologies. (Rahaim & Little, 2015; Basnayaka & Haas, 2017).

VLC is an optical wireless communication technology that uses the visible light spectrum to transmit data (Ghassemlooy et al., 2017). It can be used in both outdoor and indoor settings. In particular, indoor VLC systems can simultaneously provide illumination and data transmission. Light-emitting diodes (LEDs), widely adopted for illumination due to their high energy efficiency and long lifetime, serve as transmitters in VLC systems. Although the visible light spectrum offers an extremely wide bandwidth (approximately 400 $THz$), the achievable communication bandwidth in practical VLC systems is limited by the switching speed of commercially available LEDs. These limitations necessitate the development of advanced transmission and multiple access (MA) techniques to enable high-speed VLC systems and support simultaneous multi-user (MU) communication.

* Yasin ALTUNBAŞ; yasin.altunbas@erzincan.edu.tr

To enhance system capacity and enable MU access in VLC systems, various MA techniques have been extensively investigated in the literature, including non-orthogonal multiple access (NOMA), space division multiple access (SDMA), and rate splitting multiple access (RSMA) (Zeng et al., 2009; Pathak et al., 2015; Naser et al., 2020; Altunbas & Turk, 2023, 2024, 2026). Among these, RSMA has recently emerged as a versatile and generalized MA framework that bridges and encompasses SDMA and NOMA in a variety of channel conditions. RSMA is a strong contender for beyond-5G and 6G systems because it provides better interference management and increased spectral efficiency (SE) by treating interference as noise and partially decoding it (Mao et al., 2022).

Each user's message in the RSMA scheme consists of a private message that can only be decoded by the intended user and a common message that can be decoded by all users. Users must resolve other users' interference to receive the common message. However, during the decoding of the private message, the interference produced by other users' private messages is treated as noise (Clerckx et al., 2020). Computational complexity and data rate can be controlled by adjusting the splitting of private and common messages. Furthermore, RSMA offers a more general transmission strategy that subsumes both SDMA and NOMA in RF systems (Clerckx et al., 2020) and VLC (Naser et al., 2020).

Upon reviewing the existing literature, it is observed that the number of studies conducted on RSMA-based VLC systems is limited. Existing studies mainly focus on power allocation strategies, sum-rate maximization, precoder design, various receiver-transmitter configurations, energy efficiency, and spectral efficiency. In (Naser et al., 2020), SDMA, NOMA, and RSMA are compared in a two-user VLC scenario in terms of weighted sum-rate (WSR), where RSMA demonstrated superior performance. In (Tao et al., 2020), a 1-layer RSMA with joint transmission (JT)-based precoding is investigated for multi-cell VLC systems under the Lambertian radiation model, where linear precoding is proposed to maximize SE based on the classical Shannon capacity formulation. Simulation results demonstrated that 1-layer RSMA achieves superior SE compared to NOMA, with performance gains dependent on user locations. In (Ma et al., 2021), a beamforming approach is proposed for RSMA-based multiple-input single-output (MISO) VLC networks. The results show that the RSMA-assisted system outperforms both SDMA and NOMA in terms of sum-rate. In (Hu et al., 2023), the authors investigate sum-rate optimization in single-input single-output (SISO) VLC systems under quality-of-service (QoS) and successive interference cancellation (SIC) constraints, and the resulting problem is addressed using a successive convex approximation (SCA) algorithm. Numerical results demonstrated that RSMA achieves performance close to NOMA with significantly lower complexity. In (Lai et al., 2023), the RSMA's downlink MU-MISO VLC systems' performance with SIC errors is analyzed, and a bit error rate (BER) expression is derived. An unequal error protection (UEP)-based rate splitting (RS) precoder is proposed to mitigate error propagation, achieving better BER results than traditional RS precoders. In (Altunbas & Turk, 2026), the performance of downlink MISO-VLC systems under practical illumination standards is assessed for scenarios with and without fairness constraints. RSMA, NOMA, and SDMA are compared using the artificial bee colony (ABC) algorithm to solve the non-convex optimization problems. The simulation results indicate that RSMA achieves higher performance than both NOMA and SDMA, while also enhancing fairness among users. A careful examination of the existing literature reveals that fairness constraints, which are critical in practical MU-VLC deployments, have not been comprehensively addressed in RSMA-based VLC systems. Ensuring user fairness while maximizing system throughput remains an open and practically relevant challenge. Table 1 summarizes the main characteristics of some related studies and highlights the main differences and contributions of the proposed work.

Motivated by these observations, this paper investigates RSMA under realistic system constraints for downlink MU-MISO indoor VLC systems. Different scenarios that may arise depending on the LEDs and the users' field of view (FoV) are taken into consideration. RSMA, NOMA, and SDMA are comparatively analyzed with respect to their sum-rate and fairness performance. For each MA scheme, sum-rate maximization problems are formulated both with and without fairness constraints. Due to the inherently non-convex nature of the resulting optimization problems, particle swarm optimization (PSO), a meta-heuristic algorithm, is employed instead of conventional deterministic or convex optimization techniques. RSMA enhances interference management through message splitting, offering flexibility to improve both sum-rate performance and user fairness. NOMA achieves high throughput by allocating different power levels to users over the same frequency resource; however, fairness management becomes more complex due to power allocation disparities. SDMA exploits spatial separation to serve users over the same frequency band, yet its fairness performance strongly depends on user spatial distribution. The comparative analysis conducted in this study provides fundamental insights

into the trade-offs among sum-rate and user fairness, thereby offering guidance on the selection of appropriate MA schemes for indoor VLC systems.

**Table 1.** Comparison of some related studies on RSMA/NOMA/SDMA-based VLC systems

| Reference | System Model | MA Scheme | Fairness Constraint | Optimization Method | Main Focus |
|---|---|---|---|---|---|
| Naser et al., 2020 | MISO-VLC | RSMA, NOMA, SDMA | No | Alternating optimization | WSR comparison |
| Tao et al., 2020 | Multi-cell VLC | RSMA, NOMA | No | Linear precoding | Spectral efficiency |
| Ma et al., 2021 | MU-MISO VLC | RSMA, NOMA, SDMA | No | Beamforming design | Sum-rate comparison |
| Hu et al., 2023 | SISO-VLC | RSMA, NOMA, OMA | Yes | SCA | Sum-rate comparison |
| Lai et al., 2023 | MU-MISO VLC | RSMA | No | Alternating optimization | BER analysis |
| This Work | MU-MISO VLC | RSMA, NOMA, SDMA | Yes | PSO | Fairness-constrained comparative analysis under overloaded user scenarios with sum-rate maximization |

The rest of this paper is structured as follows: In Section 2, the system model is displayed. In Section 3, the PSO algorithm is introduced, and the optimization problems for RSMA, NOMA, and SDMA are formulated. The numerical results are discussed in Section 4, and the paper is concluded in Section 5.

## 2. System model

In this section, the mathematical model of an RSMA-based MU-MISO VLC system is presented. To investigate different communication scenarios arising from the LED radiation characteristics and the users' FoV, a downlink MU-MISO VLC system is considered. Figure 1 illustrates the downlink VLC system model consisting of three LED transmitters and two users.

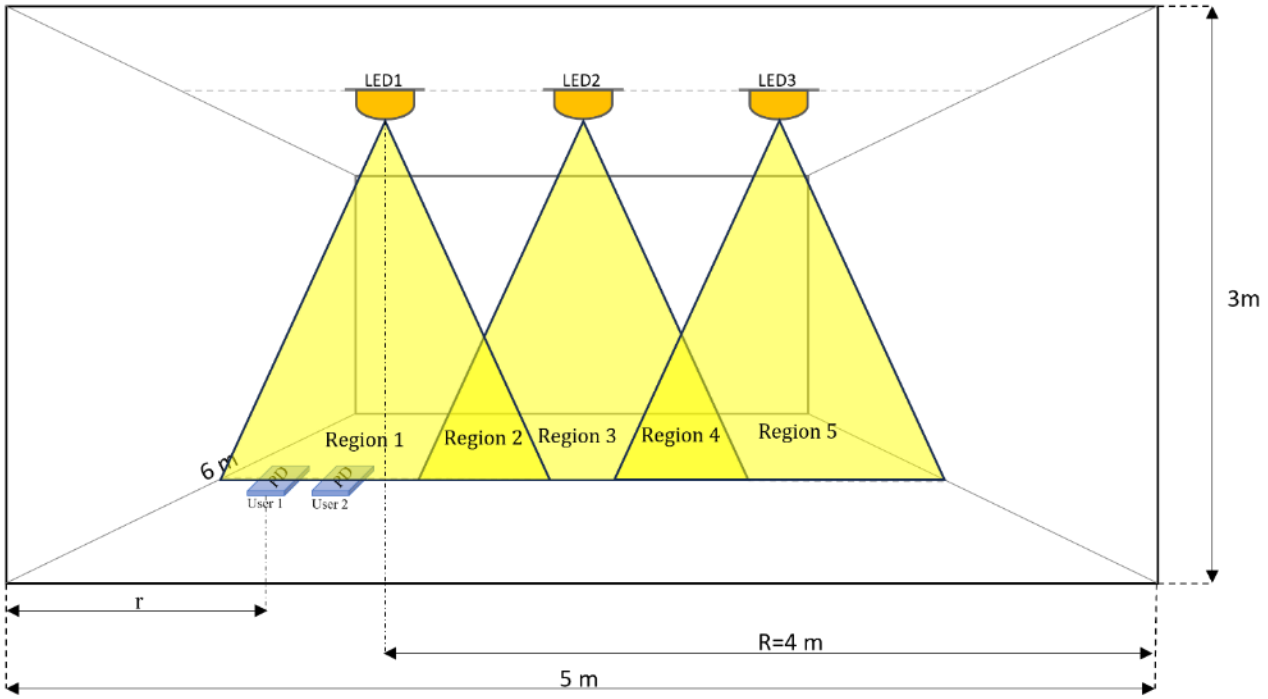


**Figure 1.** Indoor downlink VLC system consisting of three LED transmitters and two users.

Figure 2 shows the architecture of a downlink VLC system using a 1-layer RS-based approach serving $M$ users. The users are indexed by the set $\mathcal{M} = \{1, \dots, M\}$, and the transmitter has $I$ LED transmitters.

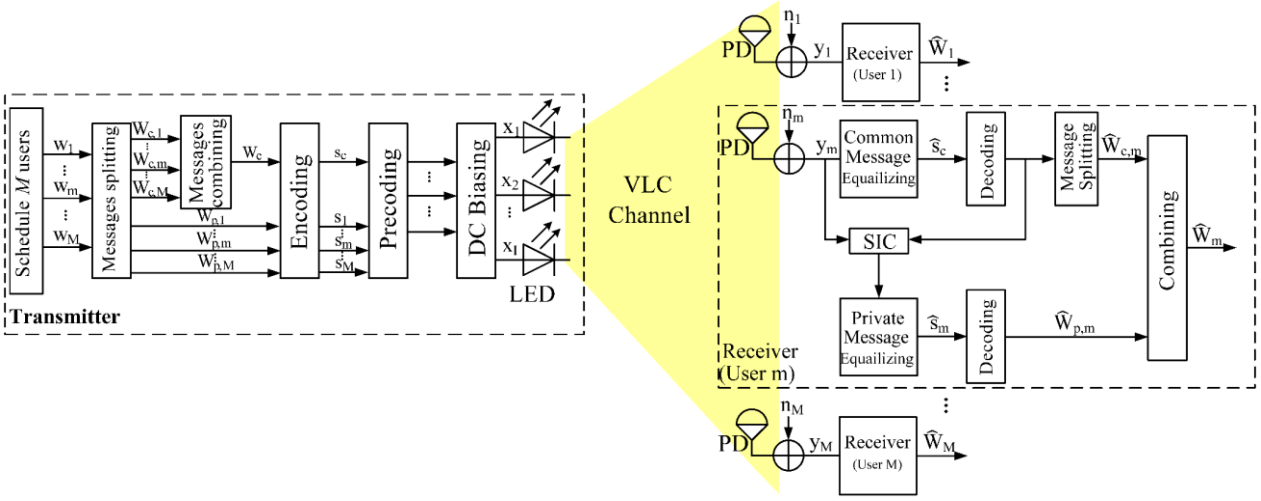


**Figure 2.** Transceiver architecture of the $M$-user MISO VLC system based on RSMA.

As illustrated in Figure 2, the message of each user $W_m$ is split into two sub-messages, namely a common sub-message $W_{c,m}$ and a private sub-message $W_{p,m}$, where the latter is intended to be decoded only by the $m$-th user. The private sub-messages of all users $W_{p,1}, \dots, W_{p,M}$ are independently encoded into private streams $s_1, \dots, s_M$, each of which is decoded only by its corresponding user. Subsequently, the common sub-messages $W_{c,1}, \dots, W_{c,M}$ of all users are combined into a single common message $W_c$, which must be decoded by all users. The common message $W_c$ is encoded into the common stream $s_c$ using a shared common codebook. Consequently, from the $M$ user messages $(W_1, \dots, W_M)$, a transmitted symbol vector $s = [s_c, s_1, \dots, s_M]^T \in \mathbb{R}^{(M+1)\times 1}$ is constructed. The precoding matrix $P = [p_c, p_1, \dots, p_M] \in \mathbb{R}^{I\times(M+1)}$, where $p_c, p_m \in \mathbb{R}^{I\times 1}$ is used to linearly precod the streams. A DC bias vector $A \in \mathbb{R}^{I\times 1}$ is added to the transmitted signal to ensure a non-negative optical signal, which is necessary for LED transmission. Accordingly, the transmitted signal $x \in \mathbb{R}_+^{I\times 1}$can be expressed as given in Equation (1).

$$x = \sqrt{P}s + A = \sqrt{p_c}s_c + \sum_{m\in\mathcal{M}} \sqrt{p_m}s_m + A \tag{1}$$

After optical-to-electrical conversion, the signal received at user $m$ can be expressed as shown in Equation (2).

$$y_m = \gamma h_m^T \sqrt{p_c}s_c + \gamma h_m^T \sqrt{p_m}s_m + \gamma \sum_{m\in\mathcal{M}, j\neq m} h_m^T \sqrt{p_j}s_j + n_m, \forall m \in \mathcal{M} \tag{2}$$

where $n_m$ is the additive noise term, $\gamma$ is the photodetector (PD) responsivity, and $h_m = \left[h_{m,1}, \dots, h_{m,I}\right]^T$ is the channel gain vector between user $m$ and the LEDs. The additive noise in VLC systems is commonly modeled as real-valued additive white Gaussian noise (AWGN) with zero mean and variance $\sigma^2 = \sigma^2_{\text{shot}} + \sigma^2_{\text{thermal}}$, where $\sigma^2_{\text{shot}}$ and $\sigma^2_{\text{thermal}}$ stand for the shot noise and thermal noise variances, respectively (Carruthers & Kahn, 1997; Altunbas & Turk, 2024). For simplicity, it is assumed that the additive noise components have the same constant noise power spectral density (PSD) $N_0$. In this case, the noise power may be written as $\sigma^2 = N_0 B$, assuming that the total system bandwidth is $B$. Furthermore, assuming a Lambertian model where reflections are neglected, the line-of-sight (LoS) optical channel gain can be calculated as given in Equation (3) (Gfeller & Bapst, 1979; Barry et al., 1993; Yazgan et al., 2018).

$$h_{LoS} = \frac{A_{PD}(k+1)}{2\pi d^2} cos^k(\varphi) T_s(\theta) g(\theta) cos\,(\theta) \tag{3}$$

where, $A_{PD}$ is the photodetector's (PD) active area, $k = \frac{-\ln 2}{\ln(\cos \Omega_{1/2})}$ is the Lambertian index, $d$ is the distance between the transmitter and the receiver, $T_s(\theta)$ is the optical filter's gain, and $g(\theta)$ is the optical concentrator's gain at the receiver. Additionally, $\Omega_{1/2}$ represents the LED's semi-angle at half power. Equation (4) defines the optical concentrator gain at the receiver, $g(\theta)$.

$$g(\theta) = \begin{cases} \frac{z^2}{sin^2\, \theta_{con}}, & 0 \leq \theta \leq \theta_{con} \\ 0, & \theta \geq \theta_{con} \end{cases} \tag{4}$$

where $z$ and $\theta_{con}$ denote the refractive index of the PD and the FoV of the receiver, respectively.

At the receiver, user $m$ first treats interference as noise and decodes the common signal $s_c$. Subsequently, SIC is used to eliminate the impact of the common signal. After the SIC operation, user $m$ treats the private signals of the other users as noise and decodes its own private message $s_m$. As a result, the achievable rate for decoding the common and private signals at user $m$ is given in Equations (5) and (6), respectively. While deriving the analytical expressions, the transmitted signal is assumed to have unit power normalization.

$$R_{c,m} = \frac{1}{2} B log_2 \left(1 + \frac{(h_m^T)^2 p_c}{\sum_{j \in \mathcal{M}} (h_m^T)^2 p_j + \sigma_m^2}\right) \tag{5}$$

$$R_m = \frac{1}{2} B log_2 \left(1 + \frac{(h_m^T)^2 p_m}{\sum_{j \in \mathcal{M},\ j \neq m} (h_m^T)^2 p_j + \sigma_m^2}\right) \tag{6}$$

The common rate must be constrained by the lowest possible common rate among all users for the common stream $s_c$ to be successfully decoded by all users. Therefore, the common rate should not exceed the value given in Equation (7).

$$R_c = min\{R_{c,1}, \dots, R_{c,M}\} \tag{7}$$

Since the sub-messages $W_{c,1}, \dots, W_{c,M}$ of the M users are contained in the common stream $s_c$, the portion of the common rate allocated to the $m$-th user is represented by $C_m$ and can be expressed as given in Equation (8).

$$\sum_{m \in \mathcal{M}} C_m = R_c \tag{8}$$

The total achievable rate of user $m$ is calculated as the sum of the private rate $R_{p,m}$ and the common rate $C_m$, as defined in Equation (9).

$$R_{m,tot} = C_m + R_{p,m},\ \forall m \in \mathcal{M} \tag{9}$$

As seen from the above expression, the achievable data rate of each user is divided into two parts: the rate of the private stream $s_m$ (private rate) and the corresponding portion of the common stream $s_c$ (common rate).

RSMA is a versatile MA method that can combine SDMA and NOMA. RSMA can be converted to SDMA by encoding each user's message exclusively as a private stream and giving the common stream zero power. In this case, the transmitted signal for SDMA can be written as given in Equation (10).

$$x = \sqrt{P} s + A = \sum_{m \in \mathcal{M}} \sqrt{p_m} s_m + A \tag{10}$$

Accordingly, the signal-to-interference-plus-noise ratio (SINR) received at user $m$ can be expressed as shown in Equation (11).

$$\gamma_{m,SDMA} = \frac{(h_m^T)^2 p_m}{\sum_{j\in\mathcal{M},j\neq m}(h_m^T)^2 p_j + \sigma_m^2} \tag{11}$$

Similarly, a two-user system is considered to illustrate how NOMA can be derived from RSMA. In this instance, the message from one user is sent via a common stream while the message from the other user is sent via a private stream. Equation (12) can depict the transmitted signal if user 1's channel gain is higher than user 2's.

$$x = \sqrt{P}s + A = \sum_{m\in\{1,c\}} \sqrt{p_m} s_m + A \tag{12}$$

Under this configuration, the SINR values at users 1 and 2 can be expressed as shown in Equations (13) and (14).

$$\gamma_{1,NOMA} = \frac{(h_1^T)^2 p_1}{\sigma_1^2} \tag{13}$$

$$\gamma_{2,NOMA} = min\left(\frac{(h_1^T)^2 p_c}{(h_1^T)^2 p_1 + \sigma_1^2}, \frac{(h_2^T)^2 p_c}{(h_2^T)^2 p_1 + \sigma_2^2}\right) \tag{14}$$

How fairly the system's capacity is allocated among users is indicated by the concept of fairness. As this value approaches 1, the difference between the users' achievable rates grows less (Manglayev et al., 2016). For the considered downlink VLC system with three LEDs and two users, the fairness index can be expressed as given in Equation (15).

$$F = \frac{\left(\sum_{i=1}^{3}\sum_{m=1}^{M} R_{i,m}\right)^2}{M\sum_{m=1}^{M}\left(\sum_{i=1}^{3} R_{i,m}\right)^2} \tag{15}$$

where $R_{i,m}$ denotes the achievable rate between the $i$-th LED and the $m$-th user.

## 3. Problem formulation

The goal of the system model under consideration is to maximize the sum-rate under the total transmit power constraint for both scenarios, with and without fairness constraints, by optimizing power control and rate allocation. Meta-heuristic optimization techniques are favored because the formulated optimization problems have a non-convex structure. In this context, PSO, which is a well-established meta-heuristic algorithm known for its reliability and effectiveness in solving complex optimization problems with high computational requirements, is adopted to obtain the solution.

### 3.1. PSO algorithm

Kennedy and Eberhart first presented the PSO algorithm in 1995 (Kennedy & Eberhart, 1995; Eberhart & Kennedy, 1995). PSO is a population-based metaheuristic optimization method that draws inspiration from the collective behavior observed in schools of fish and flocks of birds when they search for food. The algorithm begins with a collection of randomly generated candidate solutions, referred to as particles, which come together to form a swarm. Every particle has a position and a velocity in the search space. Each particle modifies its trajectory during the optimization process by taking into account two crucial pieces of information: the best position found by the swarm as a whole (global best, $gbest$) and its own best position encountered thus far (personal best, $pbest$). The swarm progressively approaches an ideal or nearly ideal solution by exchanging this information among the particles. Every particle's position and velocity are updated at each iteration. The velocity update mechanism for the $n$-th particle at iteration $t$ can be expressed as given in Equation (16).

$$V_n^{t+1} = \omega V_n^t + c_1 r_1 (pbest_n^t - X_n^t) + c_2 r_2 (gbest^t - X_n^t) \tag{16}$$

where $\omega$ denotes the inertia weight, $c_1$ and $c_2$ are the acceleration coefficients, and $V_n^{t+1}$ is the velocity vector of the $n$-th particle at iteration $(t+1)$. Random numbers with a uniform distribution within the interval $[0, 1]$ make up the parameters $r_1$ and $r_2$. Additionally, $X_n^t$ shows the current position of the $n$-th particle at iteration $t$, $gbest^t$ indicates the best position found by the entire swarm, and $pbest_n^t$ represents the best position found by the $n$ −th particle up to iteration $t$. Each particle's position is updated by adding the velocity vector to its current position after the velocity has been updated. This can be expressed as shown in Equation (17).

$$X_n^{t+1} = X_n^t + V_n^{t+1} \tag{17}$$

where $X_n^{t+1}$ denotes the updated $n$-th particle's location at iteration $(t+1)$. These steps are repeated iteratively until a stopping criterion, such as reaching the maximum iteration count or achieving a desired objective value, is satisfied.

The non-convex optimization problems designed for the RSMA, NOMA, and SDMA schemes are solved in this study using the PSO algorithm implemented in MATLAB. In this study, PSO is preferred due to its suitability for solving non-convex optimization problems. Compared to conventional convex optimization techniques, PSO provides a flexible optimization framework for multi-variable optimization problems. In addition, PSO is widely utilized because of its capability to avoid local optima and achieve stable convergence performance.

### 3.2. Problem formulation for RSMA

This section formulates a sum-rate maximization problem for a downlink MU-MISO RSMA-based VLC system under transmit power and fairness constraints. The corresponding optimization problem is presented in Equation (18).

$$R_{T,RSMA} = \max_{p_m,\, C_m} \sum_{m=1}^{M} \left[ C_m + \frac{1}{2} log_2 \left( 1 + \frac{(h_m^T)^2 p_m}{(h_m^T)^2 \sum_{j=1, j\neq m}^{M} p_j + \sigma_m^2} \right) \right] \tag{18}$$

$$\sum_{m=1}^{M} C_m \leq \frac{1}{2} log_2 \left( 1 + \frac{(h_m^T)^2 p_c}{(h_m^T)^2 \sum_{j=1}^{M} p_j + \sigma_m^2} \right) \tag{18a}$$

$$p_c + \sum_{m=1}^{M} p_m \leq P_{max} \tag{18b}$$

$$F \leq \frac{\left( \sum_{i=1}^{3} \sum_{m=1}^{M} R_{i,m} \right)^2}{M \sum_{m=1}^{M} \left( \sum_{i=1}^{3} R_{i,m} \right)^2} \tag{18c}$$

$$C_m \geq 0,\ p_m \geq 0,\ p_c \geq 0, \forall m \in \mathcal{M} \tag{18d}$$

where the LED's maximum transmit power is denoted by $P_{max}$. Every user is guaranteed to be able to decode the shared message thanks to constraint (18a). (18b) limits the total transmit power by $P_{max}$, and (18c) guarantees the desired fairness level when fairness is taken into account by incorporating the fairness constraint into the optimization problem.

### 3.3. Problem formulation for NOMA

In a NOMA-based VLC system, multiple users share the same transmission resources through power-domain multiplexing. Accordingly, the downlink MU-MISO-NOMA VLC system's sum-rate maximization issue, subject to transmit power, fairness, and decoding order constraints, can be formulated as given in Equation (19).

$$R_{T,NOMA} = \max_{p_{i,m}} \sum_{m=1}^{M} \sum_{i=1}^{3} \frac{1}{2} log_2 (1 + SINR_{i,m}) \tag{19}$$

$$\sum_{m=1}^{M} p_{i,m} \leq P_{max} \tag{19a}$$

$$h_{i,1} \geq h_{i,2} \Rightarrow U_{i,1} < U_{i,2} \wedge h_{i,2} \geq h_{i,1} \Rightarrow U_{i,2} < U_{i,1} \tag{19b}$$

$$F \leq \frac{\left(\sum_{i=1}^{3}\sum_{m=1}^{M} R_{i,m}\right)^2}{M\sum_{m=1}^{M}\left(\sum_{i=1}^{3} R_{i,m}\right)^2} \tag{19c}$$

$$p_m \geq 0 \tag{19d}$$

where constraint (19b) represents the users' decoding order according to their channel gains in relation to the $i$-th LED. Constraint (19c) is incorporated into the optimization problem when the fairness constraint is taken into account.

### 3.4. Problem formulation for SDMA

In the SDMA-based VLC system, users are spatially separated through beamforming. For the downlink MU-MISO-SDMA VLC system, the corresponding sum-rate maximization problem, subject to fairness and transmit power constraints, is formulated as given in Equation (20).

$$R_{T,SDMA} = \max_{p_m} \sum_{m=1}^{M} \left[\frac{1}{2} log_2\left(1 + \frac{(h_m^T)^2 p_m}{(h_m^T)^2 \sum_{j=1, j\neq m}^{M} p_j + \sigma_m^2}\right)\right] \tag{20}$$

$$\sum_{m=1}^{M} p_m \leq P_{max} \tag{20a}$$

$$F \leq \frac{\left(\sum_{i=1}^{3}\sum_{m=1}^{M} R_{i,m}\right)^2}{M\sum_{m=1}^{M}\left(\sum_{i=1}^{3} R_{i,m}\right)^2} \tag{20b}$$

$$p_m \geq 0 \tag{20c}$$

Constraint (20b) is incorporated into the optimization problem when the fairness constraint is considered.

It can be observed that the formulated sum-rate maximization problems for RSMA, NOMA, and SDMA are non-convex since the coupled variables are present in both the constraints and the objective functions. As a result, obtaining the global optimal solution using conventional convex optimization techniques becomes challenging. Therefore, a meta-heuristic optimization approach, the PSO algorithm-based, is adopted to efficiently solve the formulated optimization problems.

## 4. Numerical results

This section displays the numerical results and the simulation setup. Both scenarios with and without fairness constraints are evaluated by comparing the sum-rate performance of an RSMA-based VLC scheme in a multi-user MISO setting against alternative approaches employing NOMA and SDMA techniques within the same framework. Table 2 lists the simulation parameters, and Table 3 lists the metaheuristic optimization algorithm's parameters. All simulations use the parameters listed in these tables, unless otherwise noted.

It is assumed that each user in the system shown in Figure 1 is positioned along a line parallel to the axes of LEDs 1, 2, and 3. User 1 and user 2 are assumed to move together, with user 2 located $0.4\ m$ ahead of user 1. As shown in the figure, the distance between the position of LED 1 and the boundary of the system coverage is denoted by $R = 4\ m$, while the distance between the starting point of the room and user 1 is represented by $r$. The normalized offset of user 1 with respect to the starting point of the room is defined as $r/R$. Due to the FoV of the LEDs, five different coverage regions are formed in the considered system. In region 1, only LED 1 provides coverage. In region 2, both LED 1 and LED 2 provide coverage. In region 3, only LED 2 provides coverage. In region 4, both LED 2 and LED 3 provide coverage. Finally, in region 5, only LED 3 provides coverage. In this study, the normalized offset value is employed to get various numerical results, and this value varies between 0 and 1. As the normalized offset increases, the region in which the users are located changes accordingly. The simulation parameters used in the study are listed in Table 2.

The PSO algorithm is used to solve the formulated optimization problems. Table 3 provides the PSO algorithm's parameter values used in the simulations.

**Table 2.** Simulation parameters

| Parameters | Value |
|---|---|
| Room size | $(5, 6, 3)\ m$ |
| Location of LED 1 | $(1, 3, 3)m$ |
| Location of LED 2 | $(2.5, 3, 3)m$ |
| Location of LED 3 | $(4, 3, 3)m$ |
| Semi-angle at half power of LED | $30°$ |
| Receiver height | $0.85\ m$ |
| PD detection area | $1\ cm^2$ |
| PD responsivity | $1\ A/W$ |
| PD FoV | $30°$ |
| Optical filter gain | 1 |
| Optical lens gain | 3 |
| Noise power spectral density | $3.9811 \times 10^{-14} A^2/Hz$ |

**Table 3.** The PSO algorithm's parameter values

| Parameters | Value |
|---|---|
| Number of particles | 20 |
| Minimum inertia weight ($w_{min}$) | 0.3 |
| Maximum inertia weight ($w_{max}$) | 0.95 |
| Random values ($r_1, r_2$) | [0,1] |
| Cognitive component ($c_1$) | 2 |
| Social component ($c_2$) | 2 |
| FITNESSFCN | Eq. (18), (19) and (20) |
| Upper bounds ($ub$) | $[1]_{1\times IM}$ |
| Lower bounds ($lb$) | $[0]_{1\times IM}$ |
| Maximum iteration | 500 |

In the first scenario, the performances of RSMA, NOMA, and SDMA are evaluated without considering fairness constraints. The achievable rates of each LED and the users are compared with respect to the normalized offset, as illustrated in Figures 3 and 4, respectively.

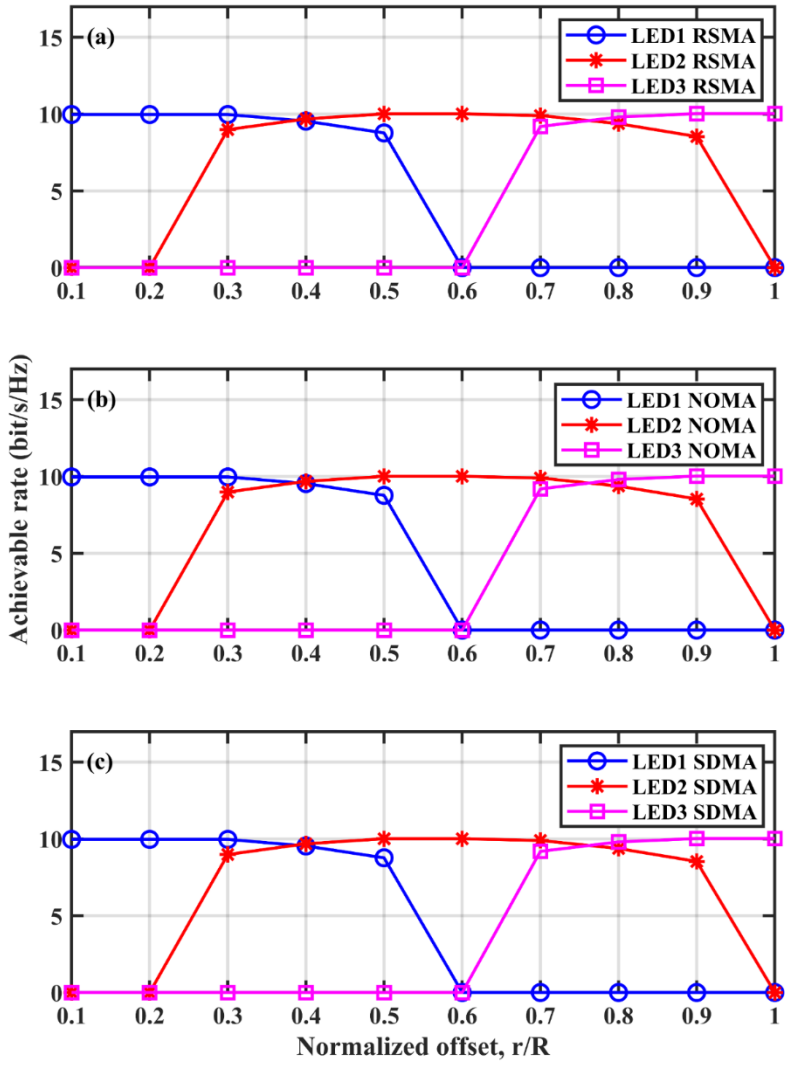


**Figure 3.** Achievable rate of each LED versus the normalized offset in the MU-MISO VLC system without fairness constraint: (a) RSMA scheme, (b) NOMA scheme, and (c) SDMA scheme.

As observed from Figures 3(a)–(c), the achievable rate of each LED exhibits a similar trend for the RSMA, NOMA, and SDMA schemes, while it varies depending on the value of $r/R$. This behavior is mainly due to the change in user regions as $r/R$ varies. More specifically, as shown in Figures 3(a)–(c), LED 1 provides data transmission within the interval $0.1 \leq r/R \leq 0.5$, LED 2 within $0.3 \leq r/R \leq 0.9$, and LED 3 within $0.7 \leq r/R \leq 1$ for all considered MA schemes.

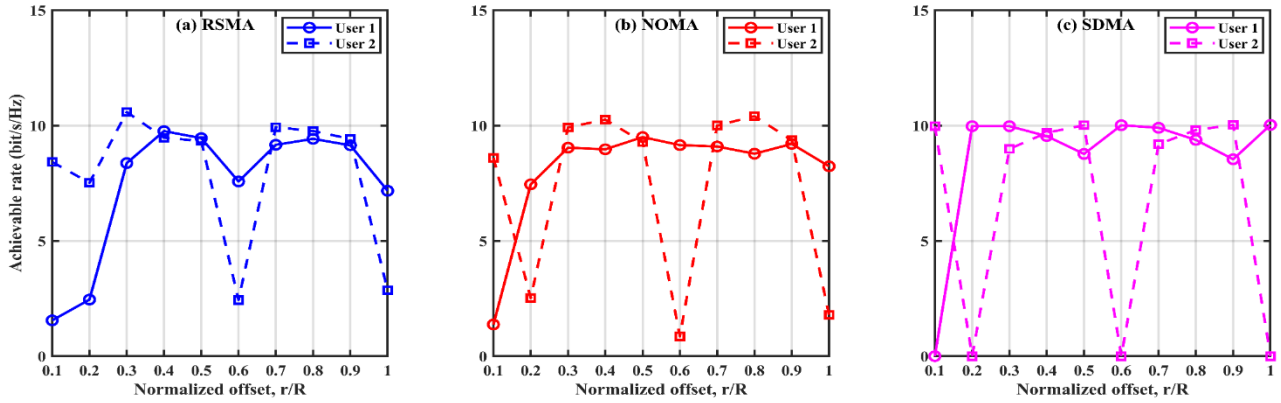


**Figure 4.** Comparing users 1 and 2 achievable rates in relation to the normalized offset for different MA schemes in the MU-MISO VLC system without fairness constraints: (a) RSMA, (b) NOMA, and (c) SDMA.

From Figure 4 (a) and Figure 4 (b), it can be observed that for RSMA and NOMA, data transmission is provided to both users for all values of $r/R$. However, as shown in Figure 4 (c), in the case of SDMA, data transmission to user 1 cannot be achieved when $r/R = 0.1$, and transmission to user 2 cannot be achieved when $r/R = 0.2$, 0.6, and 1. This behavior arises from the operating principle of the SDMA scheme. In general, Figures 3 and 4 show that when $r/R$ is set to 0.1, 0.2, 0.6, and 1, data transmission to the users is provided from only a single LED.

Figure 5 is obtained by summing the achievable rate of LEDs 1, 2, and 3 shown in Figures 3, or equivalently, by summing the achievable rate of users 1 and 2 shown in Figure 4 for the RSMA, NOMA, and SDMA schemes.

As can be seen from Figure 5, the RSMA, NOMA, and SDMA schemes achieve the same sum-rate. However, when SDMA is used, data transmission is provided only to one user in some regions where users receive signals from a single LED. In addition, the fairness values corresponding to the sum-rates shown in Figure 5 are presented in Figure 6.

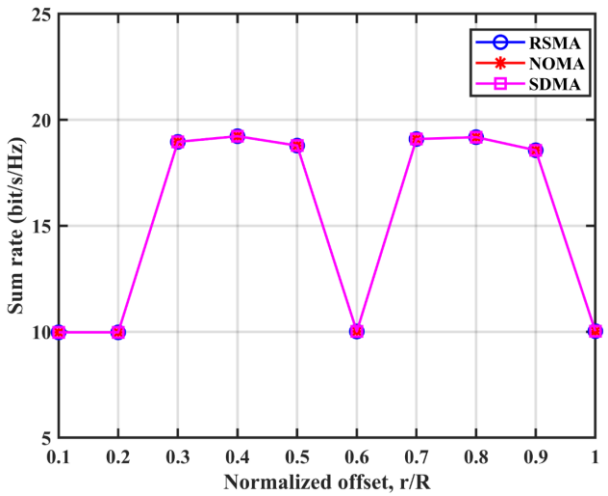


**Figure 5.** Comparison of the sum-rate with respect to the normalized offset for different MA schemes without fairness constraint.

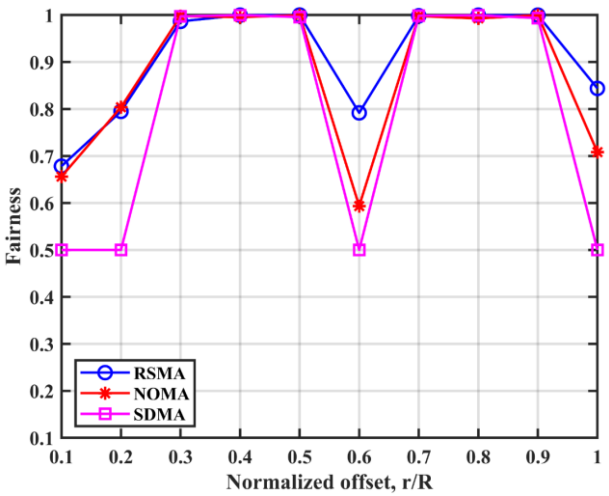


**Figure 6.** Comparison of the fairness values obtained for different MA schemes without fairness constraint with respect to the normalized offset.

The RSMA scheme provides fairer data transmission than the NOMA and SDMA schemes, as shown in Figure 6, while the NOMA scheme provides fairer data transmission than the SDMA scheme.

In the second scenario, the analyses are performed by considering a fairness constraint for RSMA, NOMA, and SDMA. For fairness values $F \cong 0.5,0.6,0.7,0.8,0.9$, and 1, the achievable rates of the LEDs with respect to the normalized offset are presented in Figure 7, the achievable rates for the user in Figure 8, and the sum-rates in Figures 9 for the RSMA, NOMA, and SDMA schemes.

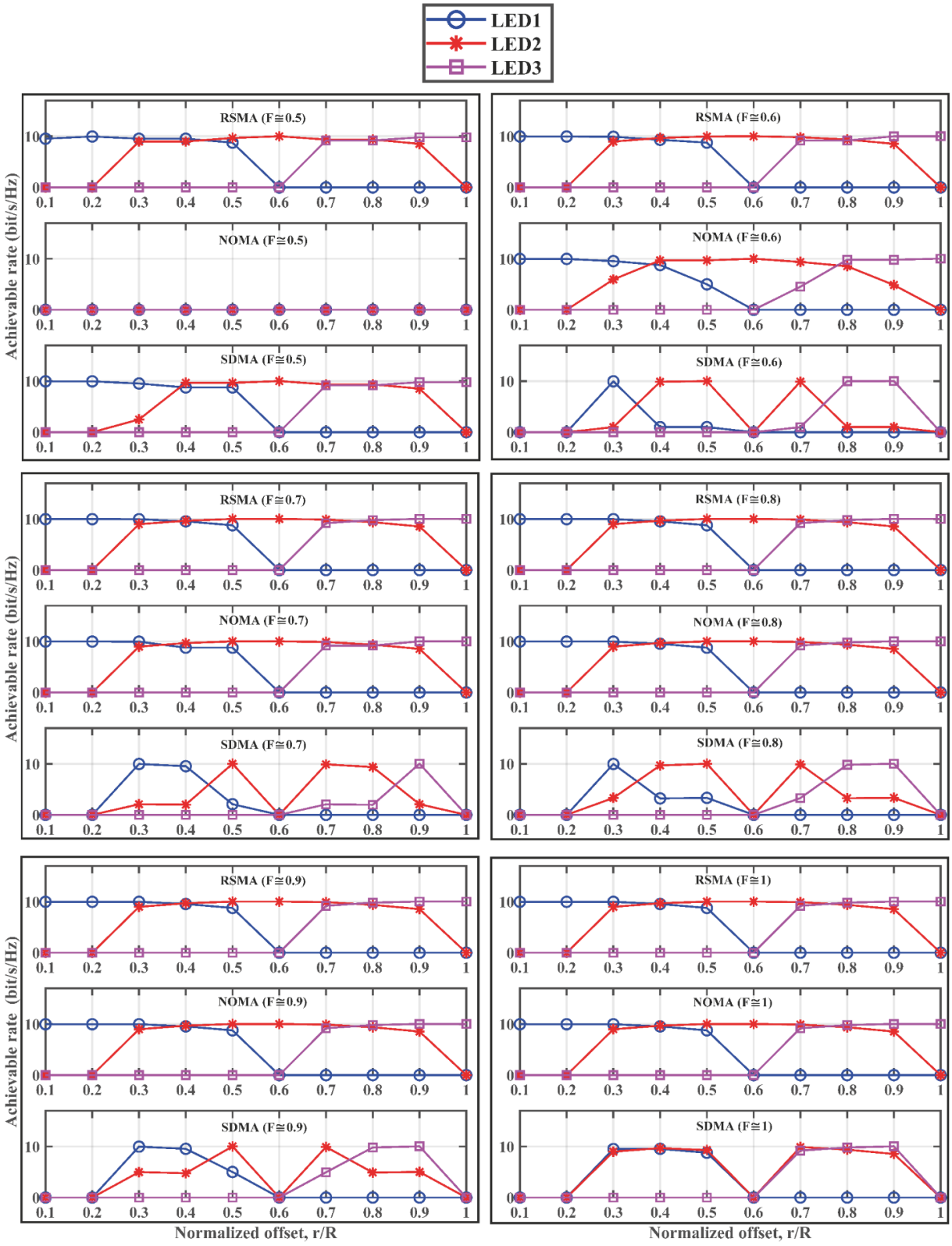


**Figure 7.** Comparison of the achievable rates of each LED with respect to the normalized offset for different MA schemes under different fairness values.

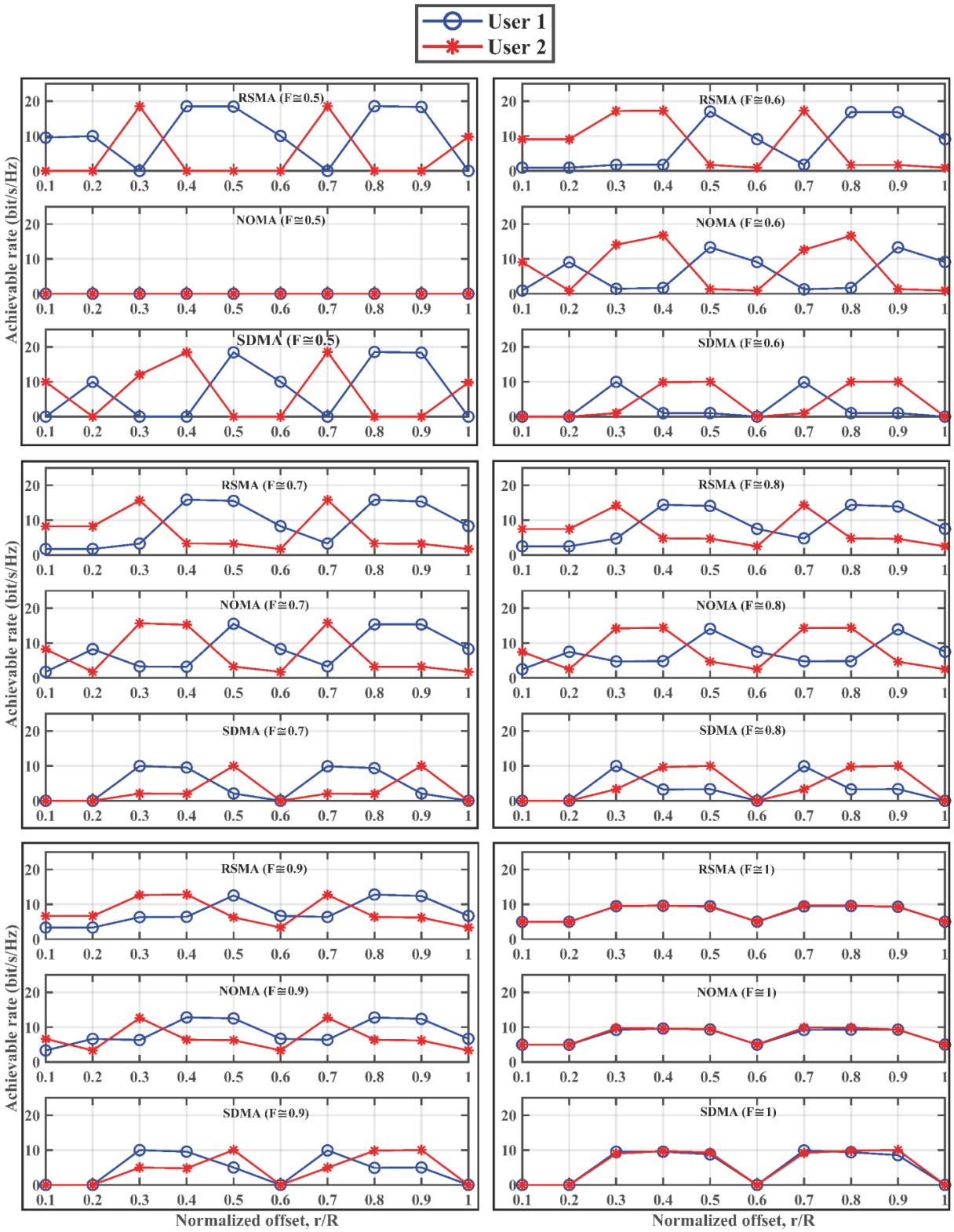


**Figure 8.** Comparing users 1 and 2 achievable rates for different MA schemes under various fairness values in relation to the normalized offset.

Figure 7 illustrates that the achievable rate curves of the LEDs in the RSMA scheme remain unchanged, regardless of the varying fairness values. In a two-user system, when $F \cong 0.5$, data transmission is provided to only one user while the other user does not receive data. Since this situation contradicts the operating principle of NOMA, it can be observed that no data transmission occurs from the LEDs in this case. As the fairness value increases, the achievable rates of the LEDs in NOMA converge to those obtained with RSMA. In a two-user system, when $F > 0.5$, both users must receive data. In overloaded scenarios where the number

of users exceeds the number of LEDs, SDMA becomes inefficient. In such cases, when $F > 0.5$, the achievable rates of the LEDs become zero in overloaded regions. However, as the fairness value increases, the achievable rates of the LEDs in SDMA approach those obtained with RSMA except in overloaded regions. From Figure 8, it can be observed that when $F \cong 0.5$, one of the users has a non-zero achievable rate while the other has a zero achievable rate for RSMA and SDMA for all values of $r/R$. Since this situation is not compatible with the operating principle of NOMA, the achievable rates for the user become zero. As the fairness value increases, both RSMA and NOMA provide non-zero achievable rates to both users for all values of $r/R$. However, in SDMA, data transmission cannot be achieved in overloaded scenarios.

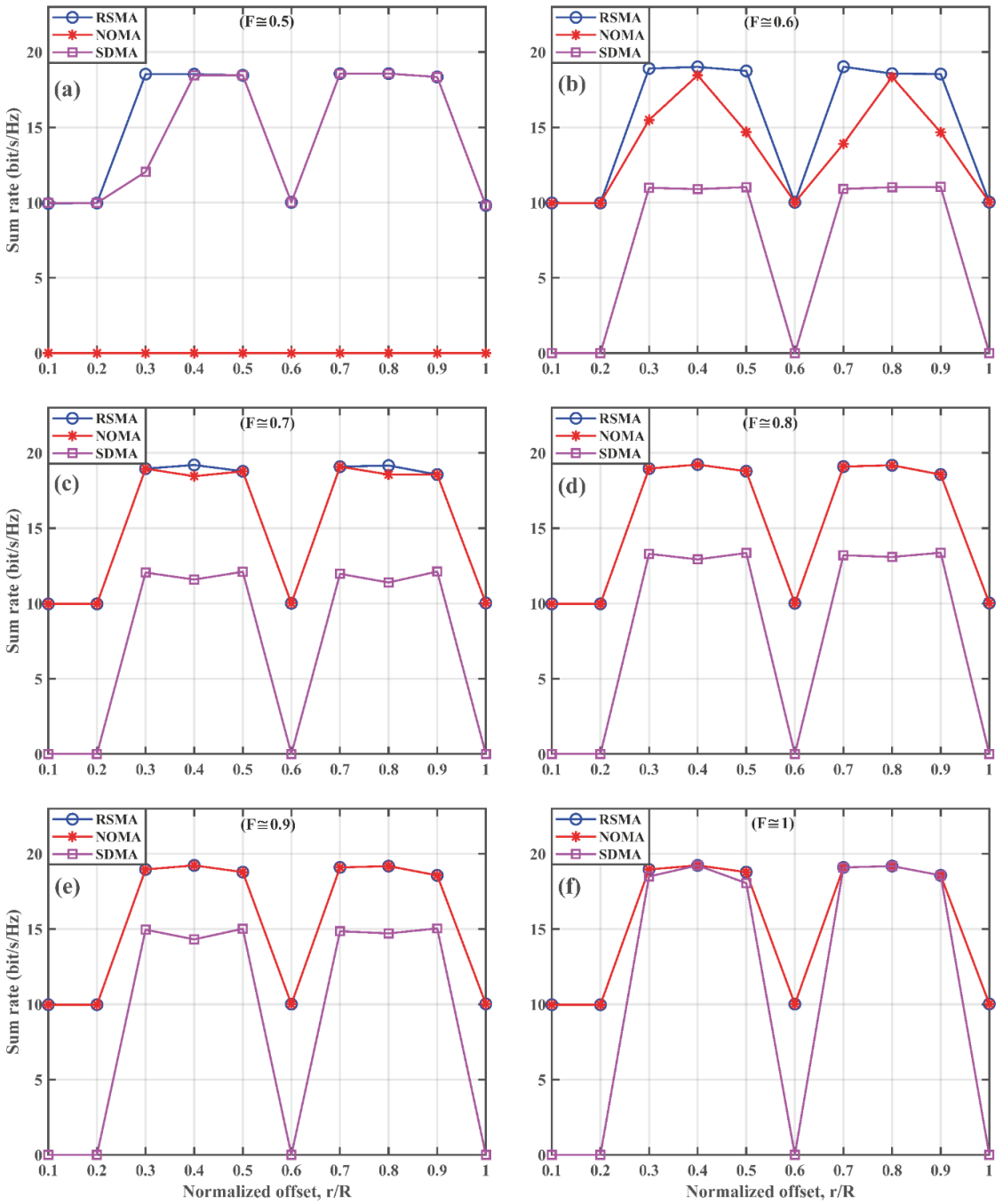


**Figure 9.** Sum-rate versus the normalized offset for different MA schemes in the MU-MISO VLC system under different fairness values: (a) $F \cong 0.5$, (b) $F \cong 0.6$, (c) $F \cong 0.7$, (d) $F \cong 0.8$, (e) $F \cong 0.9$, and (f) $F \cong 1$.

Figures 9 (a)–(f) are obtained by summing the achievable rates of LEDs 1, 2, and 3 shown in Figure 7, or equivalently, by summing the achievable rates of the users shown in Figure 8. As observed from Figures 9(a)–(f), the curves corresponding to RSMA remain unchanged for different fairness values. This behavior can be

attributed to the inherent structure of RSMA, where the rate-splitting mechanism enables a flexible allocation between common and private messages. As a result, RSMA can inherently adapt to fairness requirements without requiring significant changes in the overall transmission strategy, thereby preserving the sum-rate performance. The fairness constraint is of significant importance in determining the transmission behavior of the considered MA schemes. As the fairness requirement increases, the achieved rates among users become more balanced, which directly affects the overall sum-rate performance and the transmission strategy. The results show that RSMA can well preserve the sum-rate performance while satisfying the fairness requirements. As the fairness parameter increases, the performance of NOMA gradually approaches that of RSMA. For SDMA, when $F \cong 0.5$, the results are approximately the same as those of RSMA and NOMA. However, for $F \geq 0.6$, the sum-rate of SDMA gradually increases, except in overloaded regions, and approaches the performance of RSMA. The results obtained show that RSMA provides a more stable transmission structure under different fairness constraints by jointly transmitting common and private messages. On the other hand, the performance of NOMA strongly depends on the power allocation strategy, and the SDMA is very sensitive to the spatial distribution of users and the number of available LEDs. Therefore, the numerical results suggest that RSMA provides a more robust tradeoff between fairness and sum-rate performance, especially in overloaded MU-MISO VLC scenarios. Overall, based on the results presented in Figures 7–9, it can be concluded that RSMA encompasses both SDMA and NOMA and acts as a bridge between these two MA schemes. In particular, the numerical results demonstrate that RSMA provides a more flexible transmission strategy compared to NOMA and SDMA. Moreover, RSMA maintains a high sum-rate performance while simultaneously achieving improved fairness among users. This behavior highlights the adaptability of RSMA in balancing rate maximization and fairness under varying system conditions. These results confirm that RSMA effectively bridges the gap between SDMA and NOMA in MU-MISO VLC systems and provides a robust MA solution for different user distribution scenarios. In order to further evaluate the effectiveness of the proposed framework, the main findings of selected VLC studies are compared with the results obtained in this work in Table 4.

**Table 4.** Comparison of the main findings of selected VLC studies and the proposed work

| Reference | Key Finding |
|---|---|
| Naser et al., 2020 | RSMA provides robust transmission performance compared to NOMA and SDMA |
| Tao et al., 2020 | One-layer RSMA improves spectral efficiency in multi-cell VLC networks and outperforms NOMA under different user distributions |
| Ma et al., 2021 | RSMA-aided beamforming provides higher achievable sum-rate performance than SDMA and NOMA under optical and electrical power constraints |
| Hu et al., 2023 | RSMA achieves performance close to NOMA with lower decoding complexity under QoS and SIC constraints |
| Lai et al., 2023 | RSMA-based precoding improves BER performance and mitigates SIC error propagation in MU-MISO VLC systems |
| This Work | RSMA maintains sum-rate performance under varying fairness constraints and overloaded MU-MISO VLC scenarios |

The main findings of RSMA/NOMA/SDMA-based VLC studies are summarized in Table 4, and a comparison with the proposed framework is provided. Unlike the existing studies that mainly focus on spectral efficiency, BER performance or conventional sum-rate analysis, the proposed work jointly evaluates the fairness and sum-rate performance in overloaded MU-MISO VLC scenarios. The obtained results demonstrate that RSMA provides a flexible and robust transmission strategy while preserving high sum-rate performance under varying fairness constraints.

## 5. Conclusions

This study examines RSMA, NOMA, and SDMA schemes for MU-MISO VLC systems both with and without fairness constraints. For both cases, optimization problems are developed to maximize the sum-rate, and the PSO algorithm is suggested as a solution. The simulation results first examined a scenario without fairness constraints and showed that the achievable rates of each LED are identical for the RSMA, NOMA, and SDMA schemes, while the achievable rates of the LEDs vary depending on the $r/R$ value. It is also observed that in the RSMA and NOMA schemes, data transmission is provided to all users for all $r/R$ values. However, in the SDMA scheme, data transmission is provided to only one of the users at certain $r/R$ values since there are more users than there are LEDs. This result indicates that the SDMA scheme becomes inefficient in overloaded

scenarios. Although the sum-rates of RSMA, NOMA, and SDMA are identical, the fairness performance differs among the schemes. In terms of fairness, RSMA provides fairer data transmission compared to NOMA and SDMA, while NOMA provides fairer transmission than SDMA. When fairness constraints are considered, the RSMA scheme maintains the same performance for different fairness values, while the NOMA scheme yields values approaching those of RSMA as the fairness level increases. In the SDMA scheme, the achievable rates increase as the fairness value increases; however, data transmission cannot be maintained in overloaded scenarios. In particular, SDMA is unable to sustain simultaneous transmission to both users for $r/R = 0.1, 0.2, 0.6,$ and $1$, while RSMA retains stable transmission performance under all the considered fairness conditions. Overall, these results demonstrate that the RSMA scheme acts as a bridge between NOMA and SDMA and generally provides a fairer data transmission strategy in MU-MISO VLC systems. The validity of this study is based on an indoor MU-MISO VLC environment with fixed LED locations under LOS channel conditions. In addition, perfect CSI and ideal SIC decoding are assumed for the RSMA and NOMA schemes throughout the analysis. The obtained results may vary under channel estimation errors and imperfect SIC conditions. Future studies may extend the proposed framework by considering imperfect CSI conditions and imperfect SIC decoding in practical VLC environments. In addition, hybrid RF/VLC scenarios and MIMO-RSMA-based VLC system models may also be investigated in future research.

**Acknowledgement**

This study is derived from the doctoral thesis entitled “Multiple Access Methods for Visible Light Communication” conducted at Karadeniz Technical University, Graduate School of Natural and Applied Sciences, Department of Electrical and Electronics Engineering.

**Author contribution**

Yasin Altunbaş: Conceptualization, Methodology, Software, Writing - original draft. Kadir Türk: Validation, Writing - review & editing, Supervision.

**Declaration of ethical code**

The authors of this article declare that the materials and methods used in this study do not require ethics committee approval and/or legal-special permission.

**Conflicts of interest**

The authors declare that there is no conflict of interest.

**References**

Altunbas, Y., & Turk, K. (2026). Sum-rate maximization for downlink rate-splitting multiple access (RSMA) in visible light communication (VLC). *Optical and Quantum Electronics*, *58*(4), 170. https://doi.org/10.1007/s11082-026-08764-w

Altunbas, Y., & Turk, K. (2023). Power Allocation for Indoor NOMA Based VLC Systems with Meta-Heuristic Optimization Algorithms. *IEEJ Transactions on Electrical and Electronic Engineering*, *18*(11), 1799–1805. https://doi.org/10.1002/tee.23906

Altunbas, Y., & Turk, K. (2024). Power Allocation with Meta-heuristic Algorithms for Indoor MIMO-NOMA Based VLC Systems. *Wireless Personal Communications*, *136*(1), 617–630. https://doi.org/10.1007/s11277-024-11340-8

Barry, J. R., Kahn, J. M., Krause, W. J., Lee, E. A., & Messerschmitt, D. G. (1993). Simulation of multipath impulse response for indoor wireless optical channels. *IEEE Journal on Selected Areas in Communications*, *11*(3), 367–379. https://doi.org/10.1109/49.219552

Basnayaka, D. A., & Haas, H. (2017). Design and Analysis of a Hybrid Radio Frequency and Visible Light Communication System. *IEEE Transactions on Communications*, *65*(10), 4334–4347. https://doi.org/10.1109/TCOMM.2017.2702177

Carruthers, J. B., & Kahn, J. M. (1997). Modeling of nondirected wireless infrared channels. *IEEE Transactions on Communications*, *45*(10), 1260–1268. https://doi.org/10.1109/26.634690

Clerckx, B., Mao, Y., Schober, R., & Poor, H. V. (2020). Rate-Splitting Unifying SDMA, OMA, NOMA, and Multicasting in MISO Broadcast Channel: A Simple Two-User Rate Analysis. *IEEE Wireless Communications Letters*, *9*(3), 349–353. https://doi.org/10.1109/LWC.2019.2954518

Eberhart, R., & Kennedy, J. (1995). A new optimizer using particle swarm theory. *MHS'95. Proceedings of the Sixth International Symposium on Micro Machine and Human Science*, 39–43. https://doi.org/10.1109/MHS.1995.494215

Gfeller, F. R., & Bapst, U. (1979). Wireless in-house data communication via diffuse infrared radiation. *Proceedings of the IEEE*, *67*(11), 1474–1486. https://doi.org/10.1109/PROC.1979.11508

Ghassemlooy, Z., Alves, L. N., Zvánovec, S., & Khalighi, M.-A. (Eds.). (2017). *Visible Light Communications: Theory and Applications* (1st ed.). CRC Press. https://doi.org/10.1201/9781315367330

Hu, J., Sun, C., Wang, J., Gao, X., & Zhao, C. (2023). Common Rate Allocation and Power Control Optimization for RSMA-Based Visible Light Communications. *2023 IEEE 97th Vehicular Technology Conference (VTC2023-Spring)*, 1–6. https://doi.org/10.1109/VTC2023-Spring57618.2023.10200448

Kennedy, J., & Eberhart, R. (1995). Particle swarm optimization. *Proceedings of ICNN'95 - International Conference on Neural Networks*, *4*, 1942–1948. https://doi.org/10.1109/ICNN.1995.488968

Lai, C., Gao, S., & Tu, G. (2023). Unequal Error Protection-based Rate-Splitting precoding for VLC systems: BER analysis. *Computer Communications*, *212*, 262–274. https://doi.org/10.1016/j.comcom.2023.10.008

Ma, S., Zhang, G., Zhang, Z., & Gu, R. (2021). *Robust Beamforming Design for Rate Splitting Multiple Access-Aided MISO Visible Light Communications*. arXiv:2108.07014. https://doi.org/10.48550/ARXIV.2108.07014

Manglayev, T., Kizilirmak, R. C., & Kho, Y. H. (2016). Optimum power allocation for non-orthogonal multiple access (NOMA). *2016 IEEE 10th International Conference on Application of Information and Communication Technologies (AICT)*, 1–4. https://doi.org/10.1109/ICAICT.2016.7991730

Mao, Y., Dizdar, O., Clerckx, B., Schober, R., Popovski, P., & Poor, H. V. (2022). Rate-Splitting Multiple Access: Fundamentals, Survey, and Future Research Trends. *IEEE Communications Surveys & Tutorials*, *24*(4), 2073–2126. https://doi.org/10.1109/COMST.2022.3191937

Naser, S., Sofotasios, P. C., Bariah, L., Jaafar, W., Muhaidat, S., Al-Qutayri, M., & Dobre, O. A. (2020). Rate-Splitting Multiple Access: Unifying NOMA and SDMA in MISO VLC Channels. *IEEE Open Journal of Vehicular Technology*, *1*, 393–413. https://doi.org/10.1109/OJVT.2020.3031656

Pathak, P. H., Feng, X., Hu, P., & Mohapatra, P. (2015). Visible Light Communication, Networking, and Sensing: A Survey, Potential and Challenges. *IEEE Communications Surveys & Tutorials*, *17*(4), 2047–2077. https://doi.org/10.1109/COMST.2015.2476474

Rahaim, M. B., & Little, T. D. C. (2015). Toward practical integration of dual-use VLC within 5G networks. *IEEE Wireless Communications*, *22*(4), 97–103. https://doi.org/10.1109/MWC.2015.7224733

Tao, S., Yu, H., Li, Q., Tang, Y., & Zhang, D. (2020). One-Layer Rate-Splitting Multiple Access with Benefits over Power-Domain NOMA in Indoor Multi-Cell Visible Light Communication Networks. *2020 IEEE International Conference on Communications Workshops (ICC Workshops)*, 1–7. https://doi.org/10.1109/ICCWorkshops49005.2020.9145287

Yazgan, A., Simsek, C., Albayrak, C., Tugcu, E., & Turk, K. (2018). Experimental Channel Measurement for Indoor Office Visible Light Communication. *2018 41st International Conference on Telecommunications and Signal Processing (TSP)*, 1–5. https://doi.org/10.1109/TSP.2018.8441287

Zeng, L., O'Brien, D. C., Minh, H. L., Faulkner, G. E., Lee, K., Jung, D., Oh, Y., & Won, E. T. (2009). High data rate multiple input multiple output (MIMO) optical wireless communications using white led lighting. *IEEE Journal on Selected Areas in Communications*, *27*(9), 1654–1662. https://doi.org/10.1109/JSAC.2009.091215